

# A Novel Approach of Quantifying Susceptibilities in Small Objects: Quantitative Diagnosis in MRI

C-Y. Hsieh<sup>1</sup>, Y-C. N. Cheng<sup>1</sup>, J. Neelavalli<sup>1</sup>, Q. Liu<sup>1</sup>, E. M. Haacke<sup>1</sup>

<sup>1</sup>Wayne State University, Detroit, Mi, United States

**Introduction:** For several neurodegenerative diseases such as Parkinson's disease, it is a challenge to quantify the susceptibilities of small *in-vivo* brain irons. On the other hand, knowing the amount of contrast agent for the molecular imaging may be important. Before these goals can be achieved, quantifying susceptibilities of small cylindrical objects is considered here. Because the least-square-fit was not an effective method for determining the susceptibilities in phantom studies [1], we invented a complex sum method for such purpose. Recently, we have studied in detail the uncertainties of the new method through simulations [2]. The simulation results are compared to gel phantom experiments.

**Simulation and Imaging Methods:** We simulated the cylindrical air tube images as they were acquired at TE=5 ms from the 1.5T MR scanner [2]. An example set of magnitude and phase images are shown in Fig. 1. Note the radius of the air tube was only one pixel. The air tube was perpendicular to the main magnetic field and was surrounded by water. The water susceptibility was assumed to be -9 ppm. The black dot at the center of the magnitude image in Fig. 1 represents the cross section of the tube. If the radius of the object is known, then the susceptibility difference and the spin density, which contains imaging parameters, can be solved through Eqs. (1) and (2). Eq. 1 shows the *i*-th complex signal is added within the *i*-th circle shown in Fig. 1. Because two unknowns are in Eq. 1, only two concentric circles are needed for solving the unknowns. Then, the susceptibility of water can be solved numerically from Eq. 2. The thermal noise is also added into the simulated images. Both the thermal noise and the systematic noise are studied separately with different tube sizes and resolutions.

For gel experiments, a capillary tube with diameter 1.615±0.003 mm was inserted into a rectangular gel phantom. The tube was perpendicular to the main field (1.5T) and was inserted in the middle of the phantom. Both coronal and sagittal images including the complex images were acquired. The echo time TE of the sequence was 5 ms and the resolution of the images were 1 mm by 1 mm by 1 mm. In order to remove eddy currents in the phase images, we took a phase profile along the long edge of the gel phantom as the reference (the middle image of Fig. 2) and subtracted the entire phase image with this profile as reference. An example phase image after removing the eddy currents is shown in the left of Fig. 2.

**Results and Discussions:** Our previous approach has applied the complex sum method using one circle [1]. However, there is one major disadvantage in the previous approach. The spin density was determined by adding the signal within a large circle. However, the radius of the large circle should be at least larger than 10 times of the object size. Even so, the susceptibility obtained from the previous approach is very sensitive to the uncertainty of the spin density. The old method is now improved by drawing two concentric circles to cancel the proton density in Eqs. 1-2. The selection of circle radii is within 10 times of the object size.

Table 1 shows the simulated susceptibilities using the complex sum method. The susceptibility comparison between 1mm and 2mm implies that high resolution MR scans could reduce the systematic errors. These systematic uncertainties listed in Table 1 are likely due to the pixelization of the simulated tube. The systematic error can be effectively eliminated if we can properly choose the circle radius such that the complex sum within the circle is equal to its analytical value. It means that the circle radius may not be an integer. Generally, we found that the systematic error is less at the choice of large circle radii than it is at the choice of small circle radii.

With only the thermal noise and an assumed SNR of 10 in simulated images, the uncertainties of the susceptibilities are calculated through the error propagation method for a variety of radius combinations. The results are listed in Table 2. We found that the uncertainty due to the thermal noise is usually high when the circle radii are large. After combining the systematic error and thermal noise in the case of tube radius 1 mm, the final uncertainties of specific selections of circle radii are within 10%. The susceptibilities obtained from the gel phantom experiments are listed in Table 3. The standard deviations of these results are roughly 5% of the mean susceptibilities. The susceptibility measurements from the gel experiments agree with the simulation results. Thus, this complex sum method shows a great promise to accurately extract local susceptibilities of small objects *in vivo*. In addition, the partial volume effect is minimized when using the complex sum method.

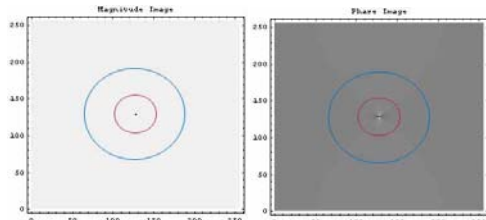


Fig. 1: Simulated MR magnitude and phase images (256x256)

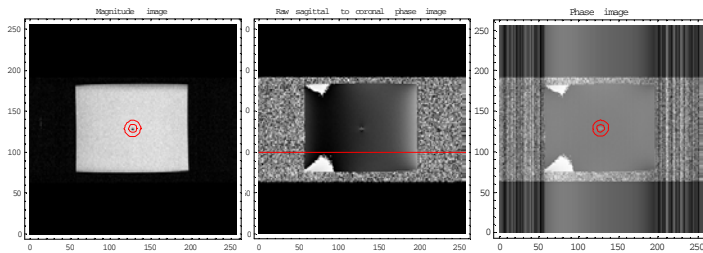


Fig. 2: The magnitude and phase images from the gel experiment

$$S_i = \sum_j M_{ij} e^{i\phi_{ij}} = \pi r_o^2 \rho_o \int_{\lambda_i}^1 \frac{J_o(0.5\gamma z T_E \chi B_o \sin^2 \theta)}{z^2} dz, i = 1, 2 \quad (1)$$

$$\frac{\sum_j M_{1j} e^{i\phi_{1j}}}{\sum_j M_{2j} e^{i\phi_{2j}}} = \frac{\int_{\lambda_1}^1 \frac{J_o(0.5\gamma z T_E \chi B_o \sin^2 \theta)}{z^2} dz}{\int_{\lambda_2}^1 \frac{J_o(0.5\gamma z T_E \chi B_o \sin^2 \theta)}{z^2} dz} \quad (2)$$

$M_{ij}$  is magnitude,  $\phi_{ij}$  is the phase.  $J_o$  is the Bessel function.  $\rho_o$  is the proton density,  $r_o$  is the tube radius, and  $\lambda_i$  is the volume fraction.

## References :

- [1] Cheng et al., ISMRM, p. 1719, 2004  
 [2] Hsieh et al., AAPM, p. 1910, 2005.

Rr1	3	4	5
Rr2	5	6	7
Tube radius 1mm	-8.578	-8.801	-8.942
Tube radius 2mm	-8.907	-8.994	-8.949

Note: Rr1 and Rr2 represent the factor of radius.

Rr1	3	4	5
Rr2	5	6	7
$\chi$ uncertainties (%)	6	8	11

Rr1	4	5	6
Rr2			
6	-8.837/-8.385		
7	-8.972/-8.585	-9.032/-9.060	
8	-9.089/-8.613	-9.274/-9.037	-9.998/-9.420
$\chi_{ave}$	-9.2/-8.93	STD( $\chi$ )	0.416/0.315